Check for updates

Hydrogeochemical characterization of groundwater in a coastal area, central western Senegal

Seyni Ndoye[1], Mathias Diedhiou[2], Helene Celle[3], Serigne Faye[2], Mohammed Baalousha[4] and Philippe Le Coustumer[5]*

[1]Département de Génie Civil, Ecole Supérieure Polytechnique, Université Cheikh Anta DIOP de Dakar, Dakar Fann, Sénégal, [2]Département de Géologie, Faculté des Sciences et Techniques, Université Cheikh Anta Diop, Dakar Fann, Sénégal, [3]Université de Bourgogne Franche-Comté, UFR Sciences et Techniques CNRS, UMR 6249 Chrono-Environnement, Besançon Cedex, France, [4]Center for Environmental Nanoscience and Risk, Department of Environmental Health Sciences, Arnold School of Public Health, University of South Carolina, Columbia, SC, United States, [5]Université de Bordeaux, B.18 av Facultés, Talence, France

One of the most serious problems affecting coastal aquifers is seawater intrusion. Senegal is currently facing an increased demand for freshwater resources due to population growth and economic development in coastal areas. In areas affected by saltwater contamination, chloride concentrations as high as 8880 mg/L were measured in groundwater samples taken from wells near the coastal zone, indicating deterioration in water quality. Our study aims to identify the zones of degradation of the water quality by determining the chemical composition of groundwater and the geochemical processes controlling the chemical patterns. Hydrogeochemical (Piper and Chadha diagrams, chloroalkaline indices, normalized bivariate plots) and multivariate statistical (Hierarchical cluster analyses) techniques were used. Forty-two groundwater samples were collected and analyzed for concentrations of major and some minor ions, electrical conductivity (EC), total dissolved solids (TDS), temperature, and pH. From samples we were able to establish a diagnosis of the very heterogeneous quality of the groundwater in this area. The average pH of the groundwater is 7.6 and about 80% of the groundwater samples have a TDS below 1000 mg/L. On the other hand, the EC values are very heterogeneous with very high conductivities in coastal areas. Approximately, 80% of the groundwater samples have a TDS less than 1000 mg/L and EC values are very heterogeneous. The dominant water types in the study area are Na-Cl water type (less than 10% of the samples) characteristic of the spatial evolution of groundwater salinization from west to east, mixed Ca-Mg-Cl due to fresh water/salt water contact and Ca-Mg-HCO$_3$ water-type (nearly 56% of the samples) to the east. A hydrogeochemical zonation of the aquifer, based on the presence of different water families allows us to visualize the highly degraded (west), mixed (center) and healthy (east) zones. Chloroalkaline indices and normalized bivariate plots show that the chemistry of groundwater is controlled mainly by water-rock interaction and evaporation processes. As water-rock interaction processes, dissolution of carbonate and evaporite, weathering of silicate, ions exchange regulates major ion chemistry.

KEYWORDS

groundwater, geochemistry, hydrochemical processes, coastal aquifer, Senegal

Introduction

The Sahel region is facing several years of persistent drought (Leroux, 1995; Gaye and Sylla, 2018). Such a drought limits the recharge of groundwater. Currently, several countries are experiencing a decline in the quantity and quality of coastal groundwater resources because of a combination of natural constraints (saline intrusion and climate change) and anthropological activities (overexploitation of water resources and increases in diffuse source pollution) (Yousfi et al., 2002; Gain et al., 2012; Hussain et al., 2019; Razack et al., 2019; Afsari et al., 2022; Wang et al., 2022; Wu et al., 2022). In Senegal, apart from regions with permanent surface water courses, the population's drinking water supply relies largely on the exploitation of groundwater. In the Mbour-Joal area located in the center-west of the country, access to water is based solely on the exploitation of groundwater collected from wells and boreholes. The reservoirs are poorly studied from a hydrogeological point of view (ARLAB, 1982; Sarr, 1982; Travi, 1988). In parallel, this coastal area is facing a significant increase in population (ANSD, 2013) due to economic opportunities (tourism as mentioned by Dehoorne and Diagne, 2008), fishing, and a pristine environment. The aquifer is therefore heavily used to meet the ever-increasing demand for drinking water and others uses. Thereby, the overexploitation of water resources leads to seawater intrusion that compromises groundwater quality. The region is characterized also by a low-lying estuary system, tidal wetlands, and denuded saline soils in the east and south. Thus, seawater has entered the hydrologic system and has been concentrated through evaporation processes to create saline surface water. Earlier studies predicted a massive saltwater intrusion after 26 years due to a rapid and excessive drop in groundwater levels (ARLAB, 1982). Travi et al. (1983) showed that the saltwater intrusion started in the west toward Ngazobil and Mbodiene (Mudry and Travi, 1995). Today, residents of the western area reported that many previously used wells have been abandoned, and newer ones are becoming brackish. This area was therefore chosen for our study. Evaluating the groundwater quality in this area, understanding the origin and the extent of saline groundwater distribution in the aquifer, and understanding the mechanism and interactions between surface water and groundwater are essential to solving water quality deterioration. Based on the hydrochemistry approach, we determine the chemical composition of groundwater (Freeze and Cherry, 1979; Faye et al., 2003; Chucuya et al., 2022; Li et al., 2022; Ren et al., 2022; Su et al., 2022; Yao et al., 2022). This study aims to (1) describe the chemical composition of groundwater and the geochemical processes controlling the chemical patterns and (2) describe the extent of saline groundwater in the region studied.
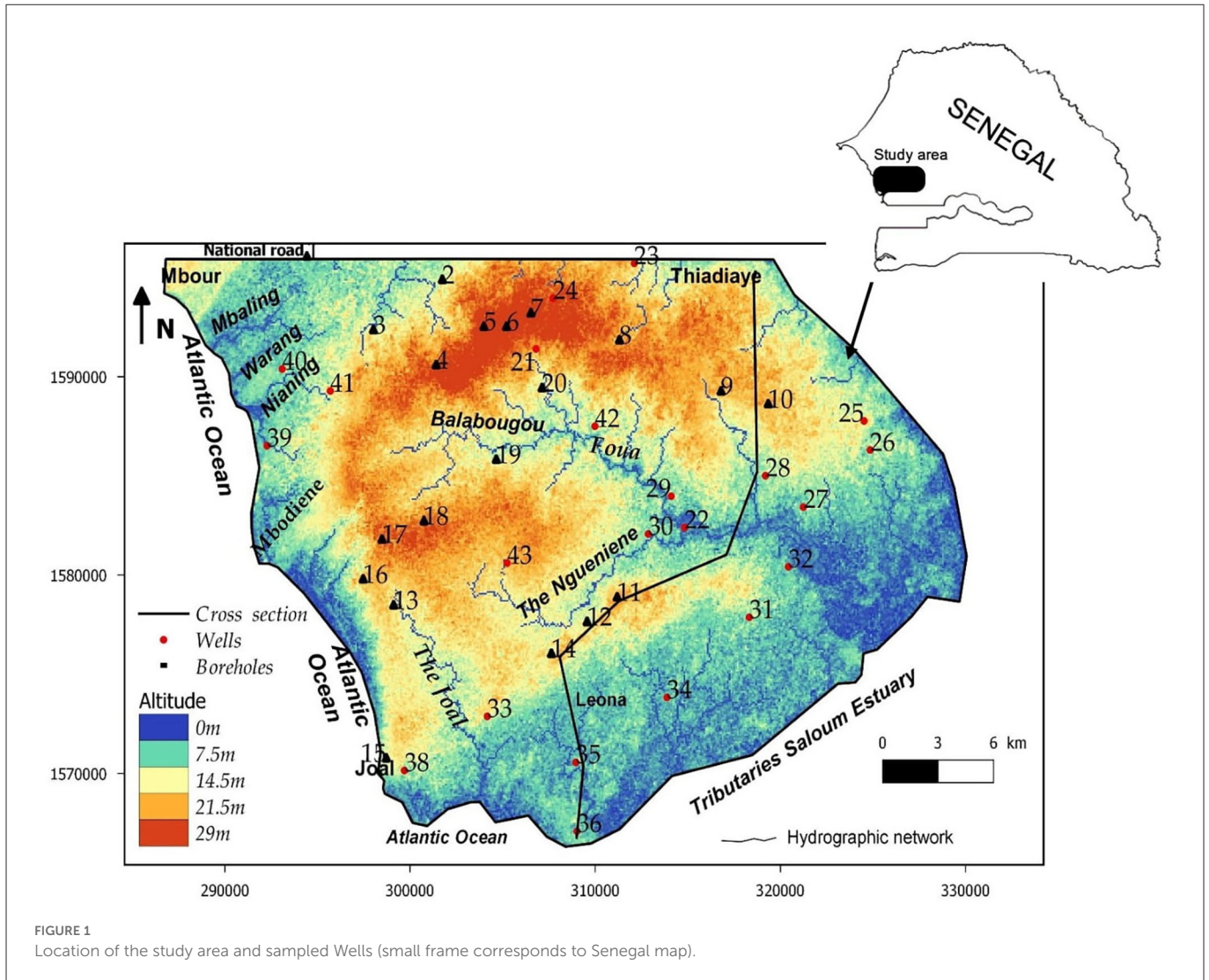
Materials and methods

The study area

The study area is located in the middle-west of Senegal between longitudes $16°38'$ to $17°00'$ W and latitudes $14°09'$ to $14°26'$N with an estimated total area of about 880 km^2 (Figure 1). Annual average precipitation and evaporation in the study area are ∼600 and 1,600 mm, respectively. The climate is of tropical type, characterized by two climatic seasons, namely, a rainy season from June to October and a dry season from November to May. The annual temperature ranges from 20°C in December to 40°C in May, and the relative humidity ranges from 60 to 96%. The topography inclines from the northwest to the southeast, and the surface elevation varies from 0 m in the estuary system to more than 20 m above mean sea level inland (Figure 1). The savannah covers almost the entire region with the exception of the littoral and estuarine zones where a particular halophyte vegetation develops. Several soils exist in the study area (Maignien, 1965; Sarr, 1982): the black to gray-black clays cover depressions; dune sands, locally called "Joor," extend well to the east, south, and extremity northwestern of the region; the saline soils, locally named "tanne"; and the black or black-gray salted soils saturated around the tributaries of the Saloum estuary.

The lithological sections (Sarr, 1999) show, at very variable levels, detrital soils with a predominance of clay and sand that constitute the layers of the Continental Terminal (Mio-Pliocene) and the Quaternary (Figure 2). The Eocene is generally characterized by marly or clayey facies enriched in limestone in the upper part (Tessier, 1954; Flicoteaux and et Lappartient, 1972). The base of Eocene consists of clayey limestone, marls and clays with quartz, flint, and phosphate (Sarr, 1982; Saint-Marc and Sarr, 1984). The Paleocene that outcrops around the town of Mbour sinks east and south-east under the Eocene formations. Paleocene is characterized by a rather great homogeneity of the calcareous and marly limestone facies, often shells (Monciardini, 1966). These shell limestones, slightly marly, karstified, or fissured, often sandstone, occupy the middle and upper horizon of the Paleocene. In the whole region, the base of the Paleocene is constituted by hard limestones and gray marly limestones, which can be sandstone (Tessier, 1954; Sarr, 1999). Beneath this formation lies the clays and sands of the Maastrichtian. Various shallow and deep aquifer systems are exploited in the study area. The Mio-Pliocene and Quaternary aquifer constituted by the clayey sands represents the marly limestone aquifer of the Upper Ypresian, the superficial system. In some areas (Figure 1: Nguéniene and Thiadiaye logs), the Eocene and Miocene-Quaternary layers form a single aquifer. In the Mio-Plio Quaternary aquifer, hydraulic conductivity is variable with mean values of 1.5×10^{-4} m/s and effective porosity of 20% (Geohydraulique OMS, 1972; Madioune et al., 2014). The deep system, essentially tapped by boreholes, wells, and wells-boreholes, is made up of the deep aquifer of the Paleocene and the Maastrichtian. The Paleocene water table is currently the most exploited with depletion or salinization in some sectors of the surface water tables (Tine et al., 2011). The hydraulic conductivities in Paleocene aquifer range from 6.6×10^{-6} to 2.0×10^{-2} m/s with a storage coefficient that varies from 1×10^{-4} to 7×10^{-2}. Currently, network functioning depends on the importance of the annual rainfall. This hydrographic network is divided into two groups: the small marigots flowing toward the ocean (MBaling, Warang, Nianing, and Mbodiene) and the tributaries of the Saloum (Figure 1). The latter (Foua, Balabougou, Joal, and Nguéniene) collect all of the water from the thalwegs. The Saloum River is the main collector of the region under marine water pressure.

Sampling, analytical methods, and data

A total of 42 samples from 22 wells and 20 boreholes (ranging in groundwater level depth from 2 to 27 m) were collected in

FIGURE 1
Location of the study area and sampled Wells (small frame corresponds to Senegal map).

polyethylene bottles in September 2019. Water bottles were rinsed three times prior to sampling, while electrical conductivity (EC), pH, and total dissolved solids (TDS) were measured in the field by a multi-parameter WTW (Model: Multi 350i/SET, Germany). Alkalinity measurements were also performed using a digital titrator (HACH). Samples for major ions analysis (Cl^-, NO_3^-, SO_4^{2-}, HCO_3^-, Na^+, K^+, Mg^{2+}, and Ca^{2+}) were collected in two 30 ml polyethylene bottles after filtration through 0.45 μm nitrocellulose membranes. Samples for cations analysis were acidified with ultrapure HNO_3^- at 70%. Bottles were filled airtight with no bubbles and kept at 4°C until analyses. Chemical analyses were conducted at the Laboratory of Chrono-Environment, University of Bourgogne Franche-Comte, France, using an ion chromatographic system (ICS) for anions and an inductively coupled plasma-mass spectrometry (ICP-MS) for cations. Ionic balance calculations in 95% of the samples were within ±10%.

Piper (1944) and Chadha (1999) diagrams were used to identify the processes controlling the groundwater hydrochemistry and groundwater types. These diagrams were constructed using DIAGRAMME Software (Simler, 2009). Multivariate statistical methods were also used to classify groundwater and interpret

hydrogeochemical processes (Brown, 1998; Wang et al., 2015). The software STATISTICA was used for statistical analysis of the hydrochemical data (StatSoft Inc, 2004). Several studies have used this technique for water types classification and determined the major factors controlling groundwater chemistry (Melloul and Collin, 1992; Farnham et al., 2000; Güler et al., 2002; Güler and Thyne, 2004; Hussein, 2004; Helstrup et al., 2007; Cloutier et al., 2008; Yidana et al., 2008; Montcoudiol et al., 2014). Among the multivariate statistical methods, the hierarchical cluster analysis (HCA) was used for this project. The HCA allows the identification of groups of groundwater samples on the basis of their similar hydrogeochemical components (Grande et al., 2003). Ward's linkage method was applied, and the Euclidean distance was chosen as the similarity measure to generate the main clusters (Güler et al., 2002).

The processes controlling groundwater hydrochemistry have also been determined by binary diagrams. The base-exchange reaction was quantified by the calculation of chloroalkaline indices (CAI) (Schoeller, 1934, 1967; Ndoye et al., 2018). Schoeller (1934) established two equations for the calculation of the chloroalkaline indices (CAI-I and CAI-II) that allow the quantification of ions'
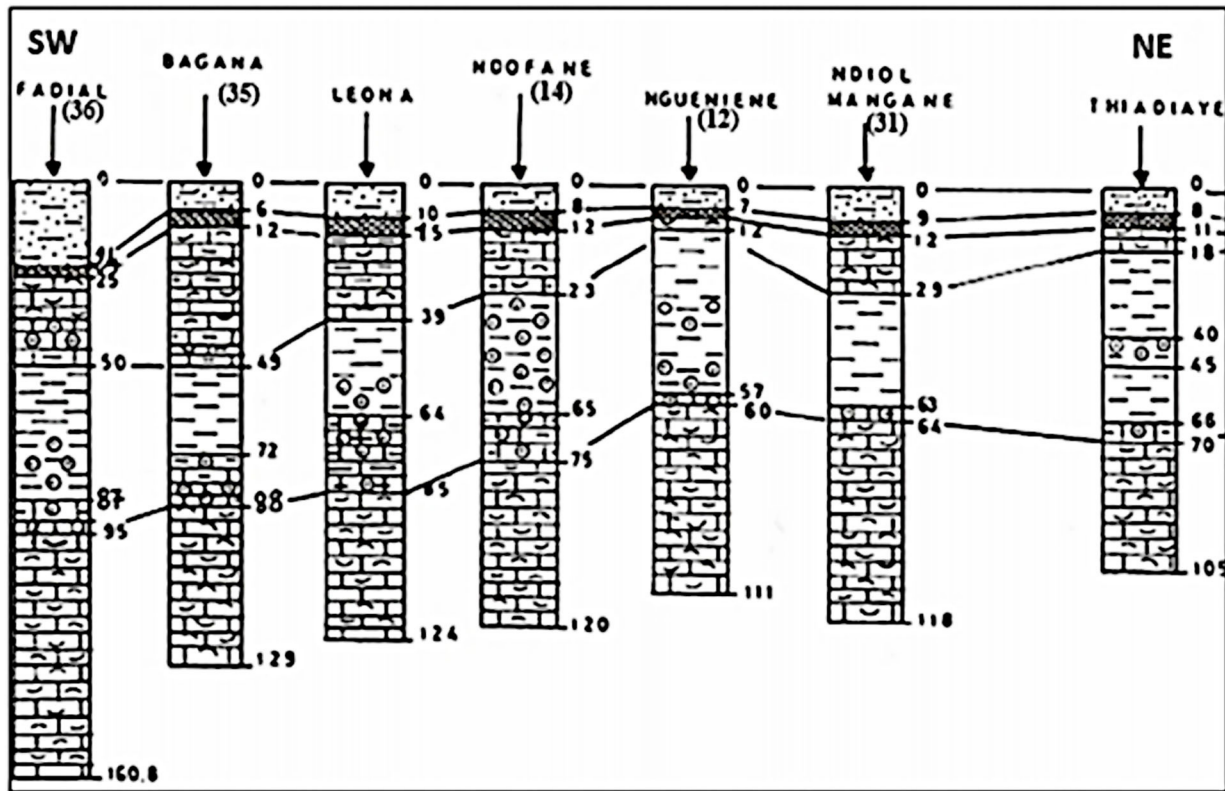
FIGURE 2
Geological cross section from Fadial to Thiadiaye (Sarr, 1999), modified. (Location of cross section is indicated in Figure 1).

exchange between groundwater and the host environment. In the following equations, the unit for the concentration of all ions is mEq/L.

$$CAI_1 = \frac{Cl^- - (Na^+ + K^+)}{Cl^-} \qquad (1)$$

$$CAI_2 = \frac{Cl^- - (Na^+ + K^+)}{HCO_3^- + SO_4^{2-} + CO_3^{2-} + NO_3^-} \qquad (2)$$

Results and discussion

General hydrochemical characteristics

The analytical results of groundwater samples are presented in Table 1. The groundwater pH ranges from 7.1 to 8.2 with an average value of 7.6, indicating neutral to slightly alkaline water. The highest

pH values are observed in the central-east zone in the localities of Guedj (43), Ngueniene (11), Ndiagamba (27), Pethemakh (9), and Ngohe (25). The electrical conductivity (EC) displays a large variability from 167 to 8,880 μS/cm, with an average value of 1,519 μS/cm (Table 2), showing that very heterogeneous water chemistry. High EC values (values >1,500 μS/cm) are observed in wells located in the coastal zone such as Ngazobil (15), Nianing (39), Sidibougou (40), Roff K. Seck (16), and Mbodiene (13). High EC values are also observed inland to Ngueniene (11), Balabougou (19), Ndiol Khokhane (31), Bagana Serere (35), and Ndiemane (18). These wells have shallow depths of 3 to 7.8 m and are located near the Balabougou and Ngueniene stream, suggesting an influence of saline surface water. Total dissolved solids (TDS) vary between 120 and 5,382 mg/L, with an average of 1,017 mg/L. Most of the samples (80%) have TDS values less than the allowable limit of 1,000 mg/L by WHO drinking water standards (WHO, 2011). The elevated EC and TDS are ascribed to the soluble electrolytes and high salinity (Brahman et al., 2013;

TABLE 1	Analytical results of groundwater samples from Mbour-Joal area.

N°	Localities	T°C	pH	TDS	EC	Ca^{2+}	Mg^{2+}	K^+	Na^+	Cl^-	NO_3^-	SO_4^{2-}	HCO_3^-
1	Keur Balla lo	31	7.7	545	910	43.9	15.7	7.8	123	278	0.2	25.4	38
2	Samane	30	7.4	649	1066	79.2	42.7	1.6	64.0	260	2.1	14.9	146
3	Mbourok Cissé	31	7.4	616	833	102	10.4	5.2	38.5	185	191	10.8	44.2
4	Bacoumbel	30	7.2	869	1156	67.8	68.7	2.5	73.3	115	15.5	47.7	435
5	Soussane	31	7.4	707	928	66.2	49.6	3.5	54.1	72.1	0.3	53.4	375
6	Ndollor	31	7.4	777	1001	70.9	48.3	5.8	69.3	79.7	10.5	46.6	411
7	Ndiouck Fissel	33	7.7	588	736	68.1	34.3	5.1	32.0	45.9	11.6	10.3	344
8	Ndioudiouf	30	7.5	569	1089	54.7	41.7	1.5	30.9	41.1	0.2	7.1	351
9	Pethemakha	31	8.0	777	999	51.9	55.8	2.7	81.9	92.2	1.9	47.2	399
10	Mbassis	32	7.7	900	1165	45.5	59.6	3.8	112	68.8	0.0	32.6	541
11	Ngenienne	31	8.0	1889	2670	137	89.7	9.0	320	452	149	291	401
12	Ngenienne Sérère	32	7.6	2103	2900	96.5	138	9.0	362	428	0.2	528	502
13	Mbodiéne Nord	30	7.7	1271	1761	85.9	91.5	5.0	163	266	0.2	163	456
14	Ndofane	31	7.5	718	881	102	12.1	0.3	71.7	58.0	17.2	37.0	375
15	Ngazobil	30	7.2	2887	4500	122	60.0	7.9	787	1107	0.9	246	512
16	Roff_K Seck	34	7.0	1207	1963	152	61.7	3.1	148	434	40.0	82.7	256
17	Roff	31	7.3	864	1246	124	43.7	1.0	64.5	186	12.9	51.0	345
18	Ndiémane	31	7.1	1578	2390	207	82.0	2.1	174	465	5.6	202	416
19	Balabougou	32	7.0	1324	2080	76.8	87.8	3.9	222	455	0.0	54.9	378
20	Diolofira oualof	31	7.4	689	878	66.0	47.7	1.8	48.3	68.4	0.4	21.0	394
21	Diolofira Sérère	30	7.6	868	1089	52.9	76.2	1.0	69.3	88.2	0.0	7.7	519
22	Keur Yérim	29	7.6	720	968	102	15.9	1.9	72.7	133	0.1	2.8	337
23	Sesséne	31	7.6	1264	2140	220	64.8	0.7	91.3	517	1.6	25.0	293
24	Diokhar Ngolem	29	7.5	697	872	81.4	44.0	0.7	36.0	62.9	18.5	6.8	405
25	Ngohé Ndofongor	31	7.8	479	565	48.0	13.0	1.0	55.1	27.5	10.8	18.7	257
26	Ngohé Pofine	32	7.7	516	625	69.4	10.1	0.5	49.2	47.2	19.8	29.9	233
27	Ndiagamba	30	8.0	452	566	45.7	24.7	0.3	35.9	41.6	14.7	30.9	204
28	Pombane	30	7.7	779	1064	34.9	62.4	2.5	96.5	132	0.3	55.8	337
29	Foua 1	30	7.7	663	871	50.6	50.1	2.7	54.5	80.1	0.3	22.3	352
30	Foua 2	30	8.0	836	1175	43.0	66.5	2.4	104	149	2.7	41.7	382
31	Ndiol Khokhane	29	7.5	1244	2030	215	13.9	1.9	166	457	19.4	67.0	263
32	Boyar Niodior	30	7.4	733	1258	116	29.8	8.4	66.3	268	16.2	21.8	175
33	Ndianda Soudiane	30	7.4	1372	1963	210	14.3	4.0	166	244	342	92.2	268
34	Thiélème	29	7.4	351	599	71.7	8.1	1.6	20.7	95.0	28.1	55.2	53
35	Bagana Sérère	31	7.6	1454	2720	222	20.1	10.7	266	788	36.2	29.8	66.5
36	Fadial	30	7.6	120	167	17.8	2.7	0.6	8.1	11.5	17.3	1.2	48.8
38	Joal Caritas	30	7.7	393	517	69.1	5.6	2.1	22.1	26.8	44.5	15.6	173
39	Nianing	30	7.3	5382	8880	562	168	1.0	1106	2626	432	433	9.4
40	Sidibougou	29	7.3	856	1696	99.0	12.7	2.8	196	499	5.1	4.3	18.9
41	Gagnabougou	29	7.4	577	958	67.0	10.6	1.5	93.9	189	55.1	13.0	113
42	Aga Biaram	30	7.6	735	968	63.7	49.7	2.0	64.7	91.6	0.7	17.9	404
43	Guedj Ngo Diagne	30	8.1	704	920	56.0	36.3	0.5	69.3	11.8	37.7	9.3	438

TABLE 2 Descriptive statistics of the physico-chemical parameters groundwater samples.

Parameters	Unit	WHO Permissible limit for drinking	Mean	Min	Max	Std dev
Temp	°C		30	29	34	1.1
pH		6.5–8.5	7.6	7.2	8.2	0.2
TDS	mg/l	1000	1017	120	5382	858
EC	μs/cm	1500	1518	167	8880	1421
Cl^-	mg/l	250	279	11.5	2626	436
NO_3^-	mg/l	50	37.2	0.0	432	88
SO_4^{2-}	mg/l	250	70.8	1.2	527	113
HCO_3^-	mg/l	300	297	9.4	541	152
Ca^{2+}	mg/l	200	103	17.8	562	90
K^+	mg/l	30	3.2	0.3	10.7	2.7
Mg^{2+}	mg/l	150	46.2	2.7	168	35.4
Na^+	mg/l	200	142	8.1	1106	201

FIGURE 3
Piper diagram of the groundwater samples of the study area.
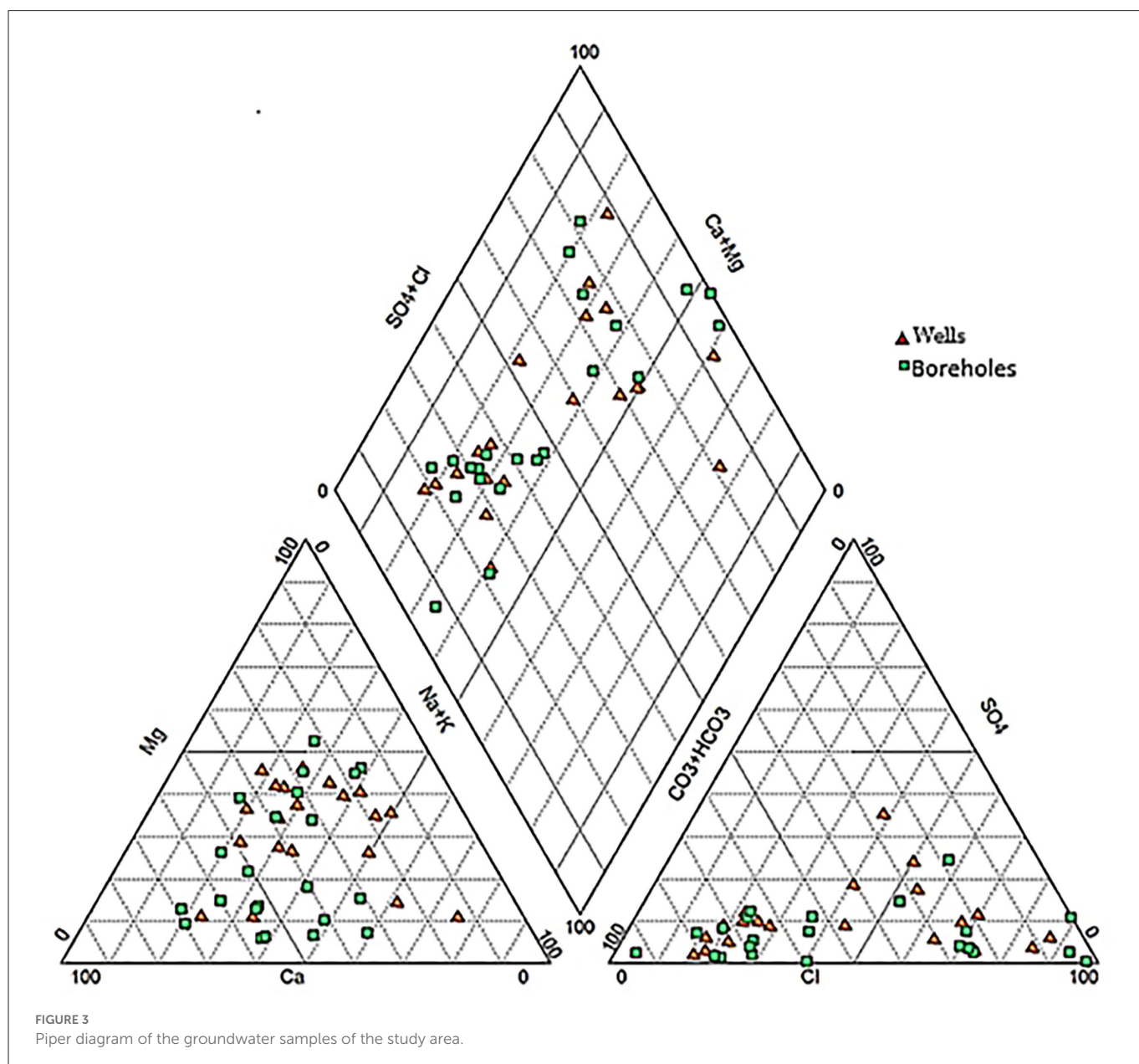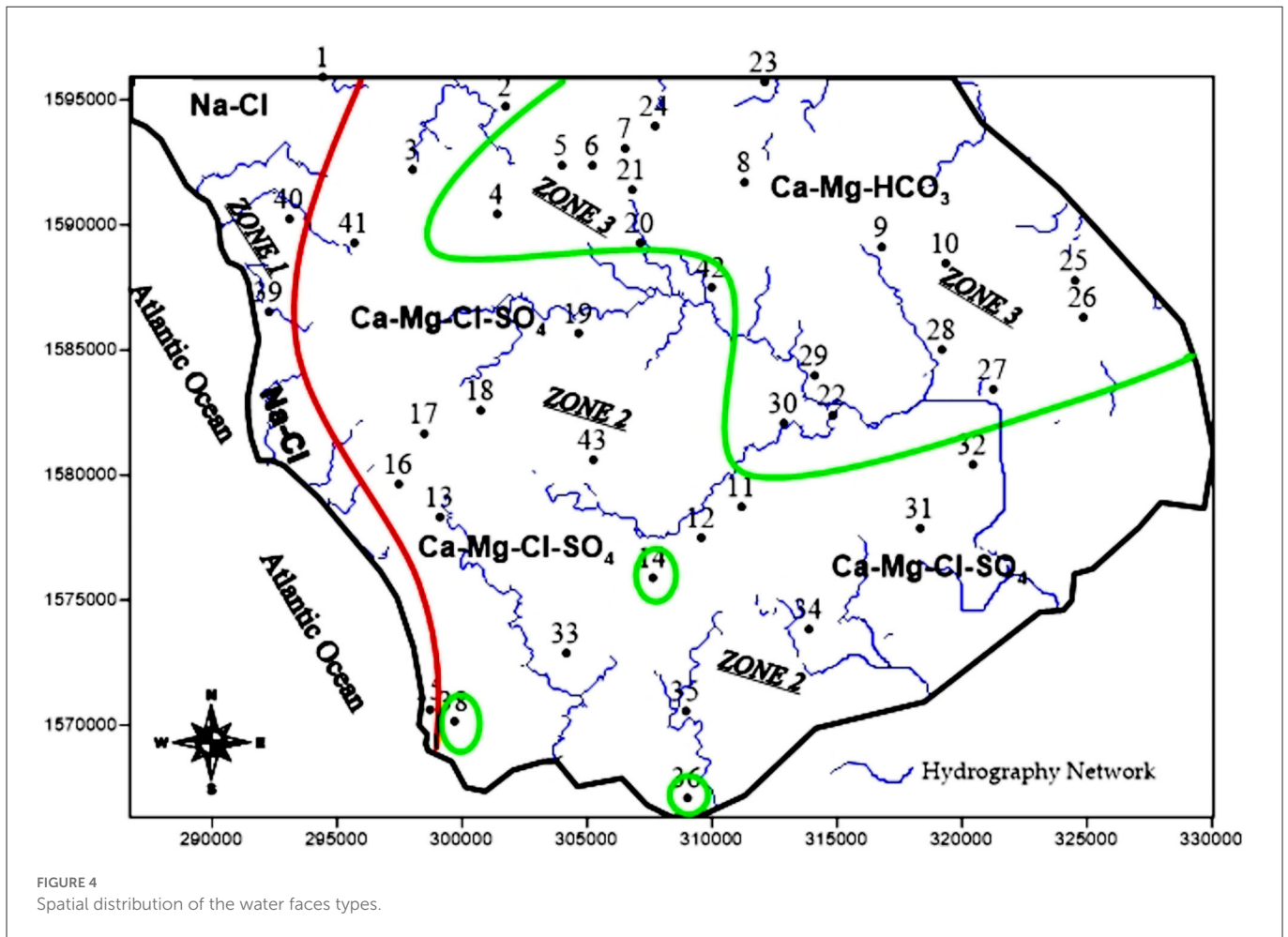
FIGURE 4
Spatial distribution of the water faces types.

Raza et al., 2016). The concentrations of Ca^{2+}, Mg^{2+}, Na+, and K$^+$ ions vary from 17.8 to 562 mg/L (mean value = 103 mg/L), 2.7 to 168 mg/L (mean value = 46.2 mg/L), 8.1 to 1,106 mg/L (mean value = 142 mg/L), and 0.3 to 10.7 mg/L (mean value = 3.2 mg/L), respectively (Table 2). The source of Ca^{2+} and Mg^{2+} in this region is the dissolution of carbonate and silicate minerals as observed in other regions (Saha and Safiur Rahman, 2020; Zhou et al., 2020). In 2020, a study by Marghade (2020) provides the origin of Na$^+$ from the dissolution of Na-containing lithogenic minerals, cation exchange, and/or mixing with seawater. Among the anions, Cl$^-$ is the dominant ion followed by HCO$_3^-$, SO$_4^{2-}$, and NO$_3^-$. The chloride concentration in the groundwater varies between 11.5 and 2,626 mg/L (mean: 280 mg/L). Dissolved chloride is common in shallow groundwater (Hem, 1992; Faye et al., 2003). This element comes from atmospheric precipitation, dissolution of salt deposits, weathering of halite and evaporite minerals (Hussien and Faiyad, 2016), and/or mixing with seawater. During dry periods, white efflorescence of salt deposits is observed. This is dissolved by rainwater and percolates toward shallow waters leading to a significant increase in the Na+ and Cl contents.

Concentrations of HCO$_3^-$ vary between 9.4 and 541 mg/L with a mean of 297 mg/L. The bicarbonate could originate from the same sources as Ca and Mg, i.e., carbonate precipitation and dissolution of silicate minerals (Belkhiri et al., 2012; Asmael et al., 2015; Chebbah and Allia, 2015; Saha and Safiur Rahman, 2020). HCO$_3^-$ also could originate from the biodegradation of organic soil compounds (Winter

et al., 1998; Magha et al., 2021). Sulfate concentrations vary between 1.2 and 527 mg/L, with a mean of 71 mg/L. Sulfate (SO$_4^{2-}$) source comes from the weathering of rocks forming minerals such as gypsum and anhydrite (Datta and Tyagi, 1996), or from the mixing of groundwater with seawater. Additionally, high sulfate concentrations may be due to the influence of leaching from sulfate-acid soils found on the "tannes" and anthropogenic activity.

The concentration of NO$_3^-$ in the groundwater ranges from 0.0 (<LOD 0.05) to 432 mg/L with a mean of 37.2 mg/L. Nitrate is a frequent contaminant in groundwater in arid and semi-arid regions and emanates from anthropogenic activities (Adimalla et al., 2019, 2020; Perez Villarreal et al., 2019; Mufur et al., 2021). High concentrations of NO$_3^-$ in the studied area are observed in Nianing (39), Ndianda (34), Ngueniene Serere (12), and Mbourock Cisse (13) and are attributed to anthropogenic local pollution from agricultural practices (fertilizers typically), improper disposal of domestic waste, animal and human waste. The concentrations of the other ions are low.

Hydrogeochemical facies and process

Piper and Chadha diagram

The Piper (1944) trilinear plot (Figure 3) reveals three main water types in boreholes and wells in the studied area: calcium magnesium
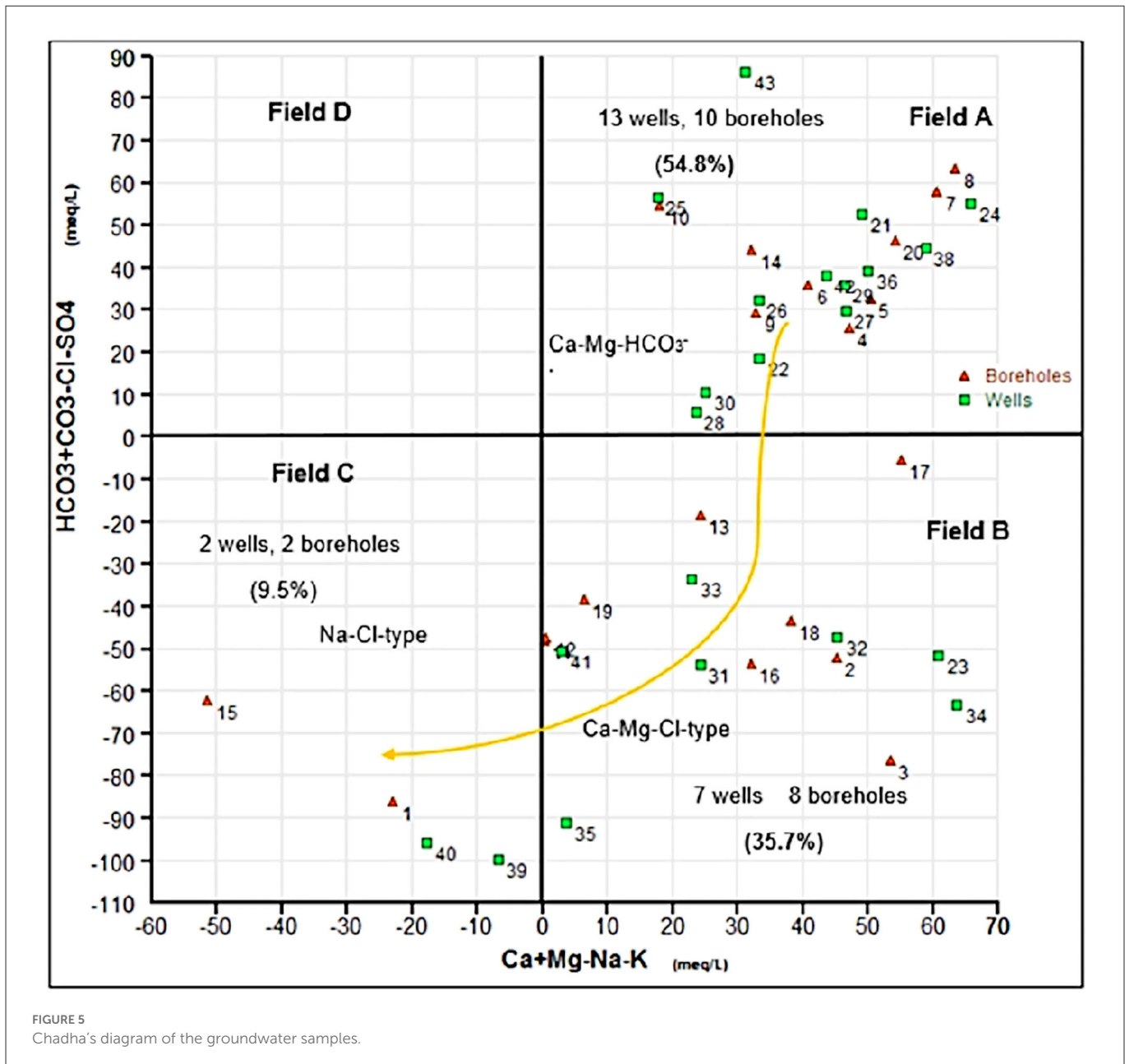
FIGURE 5
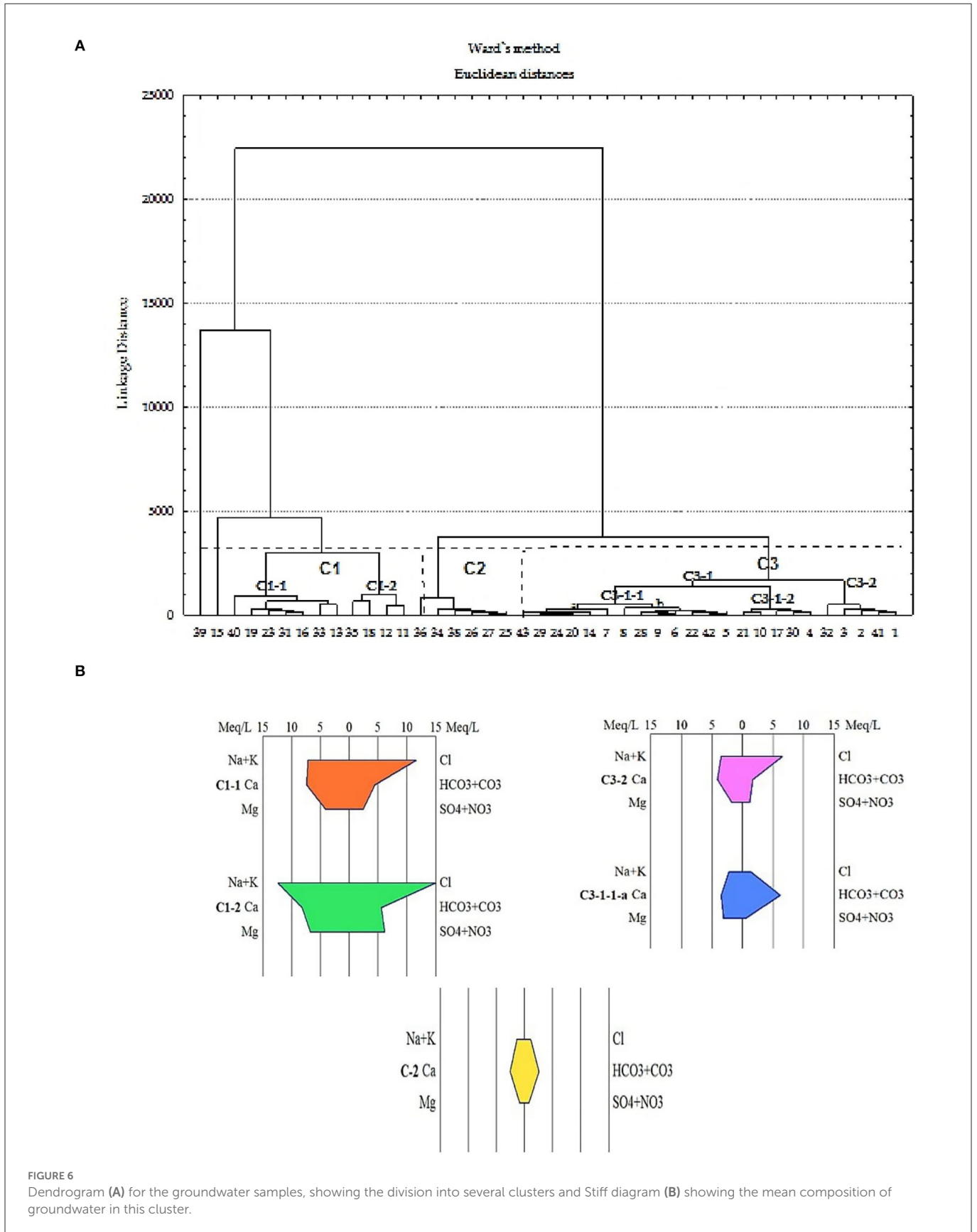Chadha's diagram of the groundwater samples.

bicarbonate (Ca-Mg-HCO₃), calcium magnesium chloride (Ca-Mg-Cl), and sodium chloride (Na-Cl). Ca-Mg-HCO₃ water type accounts for 50% of analyzed samples. They are found essentially in zone 3 (Figure 4) located in the north-east of the studied area. This water type is attributed to the dissolution of calcite and dolomite. The sodium chloride (Na-Cl) water type is located in the vicinity of the sea, zone 1. This water type may originate from brackish water of surface and/or seawater intrusion. The Ca-Mg-Cl-SO₄ water type is encountered in the wells located in the middle part of the area (zone 2). For most groundwater samples in zone 2, the dominant cation Ca^{2+} and the dominant anion is Cl^-.

Chadha diagram (Chadha, 1999) is used to verify the classification of water type (Figure 5). This diagram defines four fields, representing four types of hydrogeochemical processes (Raza et al., 2016; Kaur et al., 2019). It allows explaining the different hydrogeochemical processes in the aquifers. The Chadha diagram shows that the data points are plotted in fields A, B, and C. The water type classification

by the Piper diagram is affirmed by results obtained with the Chadha plot. In this plot, 54.8% of the samples are represented by Ca-Mg-HCO₃ water type (Field A), 35.7% of the samples are represented by Ca-Mg-Cl water type (Field B), and 9.5% of the samples are represented by Na-Cl water type (Field C). Ca-Mg-HCO₃ water type reflects the dissolution of carbonates and/or the alteration of silicates. The facies Ca-Mg-Cl type in our case reveals a mixing zone where the dissolution process was observed (A type) combined with the diffusion of brackish waters. The facies Na-Cl can find its origin in the evaporation process or mixing with seawater.

Hierarchical cluster analyses (HCA)

Using HCA, three major clusters C_1, C_2, and C_3 including four subclusters C_{1-1}, C_{1-2}, C_{3-1}, and C_{3-2} are identified (Figure 6A). The C_1 cluster consists of two subclusters C_{1-1} and C_{1-2} and

FIGURE 6
Dendrogram (A) for the groundwater samples, showing the division into several clusters and Stiff diagram (B) showing the mean composition of groundwater in this cluster.

represents 28.5% of the water samples. The C_{1-1} subcluster includes wells 15, 16, 19, 23, 31, 33, and 40, and the C_{1-2} subcluster includes wells 11, 12, 13, 18, and 35. The mean EC is 1,948 µS/cm for C_{1-1} (Ca-Cl) and 2,670 µS/cm for C_{1-2} subcluster (Na-Cl). This water type is characteristic of highly saline water.
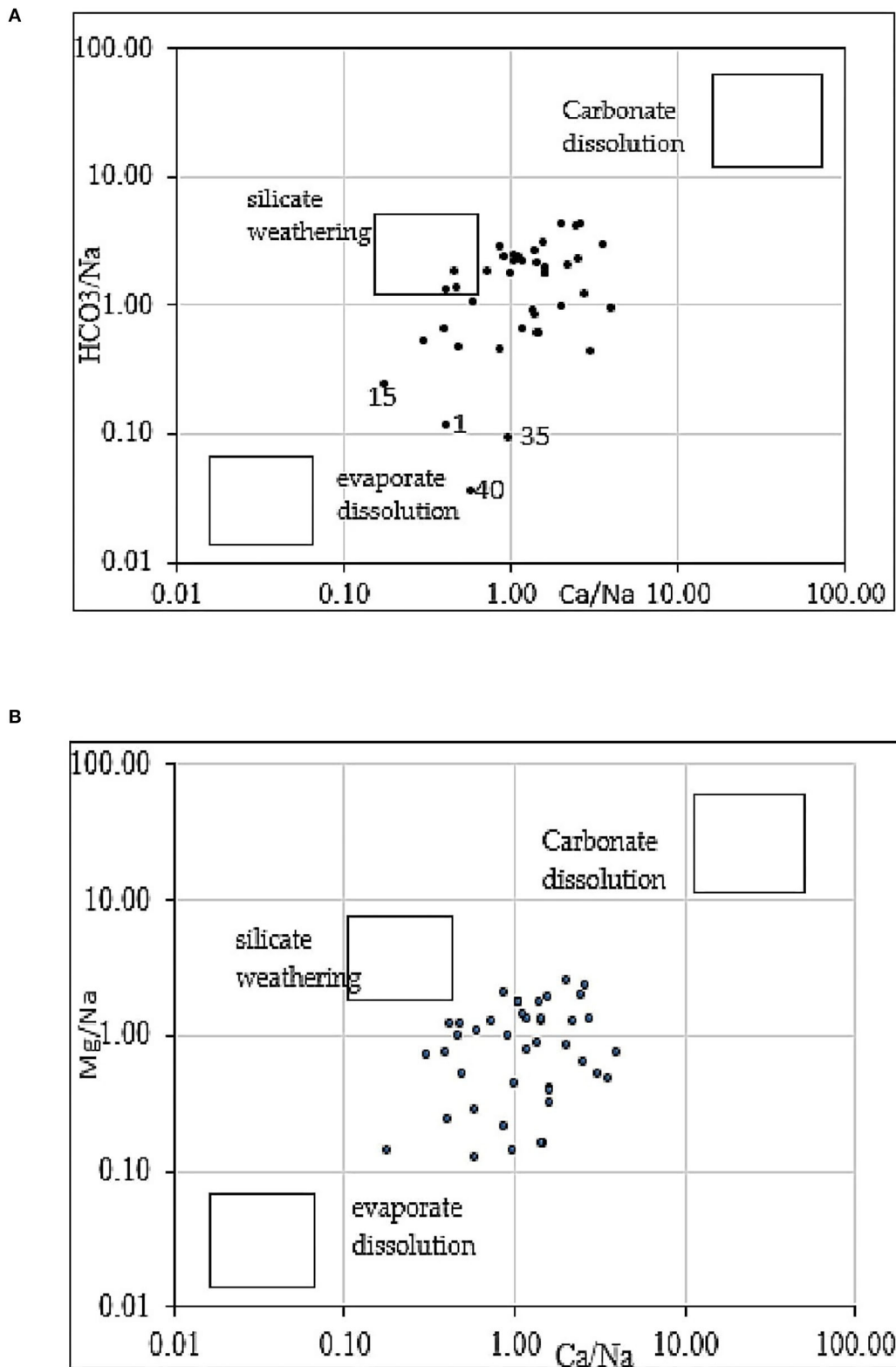
FIGURE 7
Bivariate mixing plots of Na-normalize Ca and HCO$_3$ **(A)** and Na-normalized Ca and Mg **(B)**.

Cluster C$_2$ includes wells 36, 34, 38, 26, 27, and 25 and accounts for 14.3% of the water samples. The mean EC for this cluster is 506 µS/cm, which is the characteristic freshwater. Groundwater in this cluster is of the Ca-HCO$_3$ type (Figure 6B). The dissolution of carbonates could be the process responsible for this type of water encountered in the central-eastern sector where the reservoir
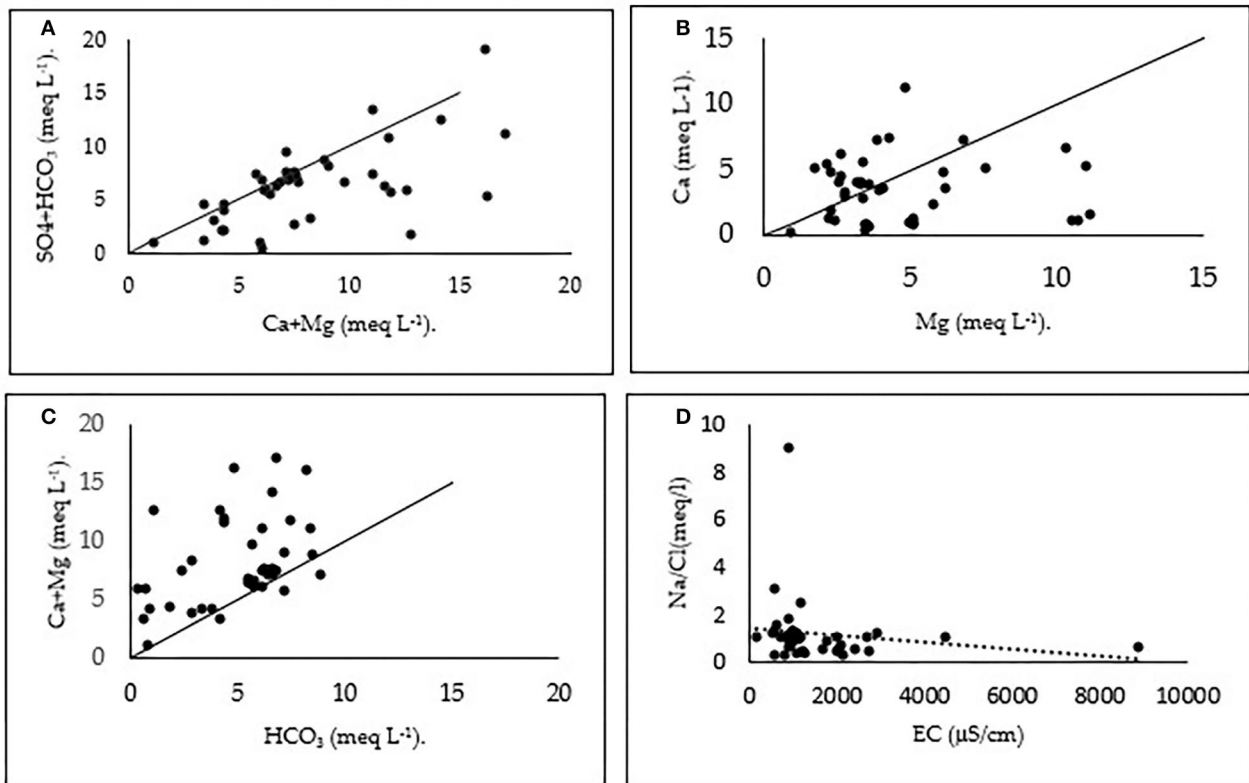
FIGURE 8
Plots of ($Ca^{2+} + Mg^{2+}$) vs. ($HCO_3^- + SO_4^{2-}$) **(A)**, Mg^{2+} vs. Ca^{2+} **(B)**, HCO_3 vs. ($Ca^{2+} + Mg^{2+}$) **(C)**, and EC versus Na/Cl **(D)**.

rock is essentially composed of argillaceous limestones flint, marl, and biogenic limestones. The third cluster (C_3) includes all the other samples divided into two subclusters C_{3-1} and C_{3-2} having a mean electrical conductivity of 1,000 µS/cm. The high chloride ion content in subcluster C_{3-2} (wells 1, 2, 3, 41, and 32) may be due to contamination by saline surface water in the vicinity of these wells (Figure 4). This type of water is interpreted by water–rock interactions as a result of dilution by salty surface water in contact with the carbonate formations of the aquifer. This water type is interpreted by water–rock interactions following dilution by salty surface water in contact with carbonate formations in the aquifer. The HCA gives a better precision of the distribution of facies and shows that the waters present a strong chemical heterogeneity unlike the Piper diagram, which illustrates three water types.

Correlation analysis of chemical parameters

A plot of Ca^{2+} vs. HCO_3^- normalized to Na (Figure 7A) (Gaillardet et al., 1999; Belkhiri et al., 2010; Liang et al., 2018) shows that groundwater is influenced by silicate weathering and carbonate dissolution for most samples. This figure also shows the influence of evaporate dissolution for some samples [Ngazobil (15), Sidibougou (40), Keur Balla (1), and Bagana Serere (35)]. A Na-normalized plot vs. Mg (Figure 7B) shows that Mg comes from the silicates weathering and evaporates dissolution.

Figure 8 shows plots of ($Ca^{2+} + Mg^{2+}$) vs. ($HCO_3^- + SO_4^{2-}$) (Figure 8A), Mg^{2+} vs. Ca^{2+} (Figure 8B), HCO_3^- vs. ($Ca^{2+} + Mg^{2+}$) (Figure 8C), and EC vs. Na+/Cl– (Figure 8D). The plot of ($Ca^{2+} + Mg^{2+}$) vs. ($HCO_3^- + SO_4^{2-}$) shows that some samples fall along the aquiline 1:1 (Figure 8A), which indicates that Ca^{2+}, Mg^{2+}, SO_4^{2+}, and HCO_3^- were derived from the dissolution of calcite, dolomite, and gypsum. This corroborates the different facies obtained using the Piper and Chadha diagrams. Many other water samples are below this line (Figure 8A), suggesting a substantial excess of ($Ca^{2+} + Mg^{2+}$) over ($HCO_3^- + SO_4^{2-}$). In these samples, reverse ion exchange is the process that explains the presence of Ca-Cl facies. This figure reveals an excess of SO_4^{2-} +HCO_3^- for some locations sampled, suggesting silicate weathering (Ndoye et al., 2018).

The plot of Mg^{2+} vs. Ca^{2+} (Figure 8B) indicates an excess of Ca^{2+} in some samples, an excess of Mg^{2+} in other samples, and a balance between Mg^{2+} and Ca^{2+} in the remaining samples. The plot of ($Ca^{2+} + Mg^{2+}$) vs. HCO_3^- (Figure 8C) shows that most of the samples are above the equiline (1:1) and only three points are below this line. Using these two plots, we can say that excess of ($Ca^{2+} + Mg^{2+}$) over HCO_3^- is balanced by Cl- and SO_4^{2-} (Su et al., 2009; Wang et al., 2013). This excess can be produced from silicate and carbonate weathering (Subramani et al., 2009). For HCO_3^-, apart from the carbonates zone, its enrichment (Figure 8C) can originate from carbonic acid-induced silicate weathering (Paul et al., 2019; Saha and Safiur Rahman, 2020) as a result of oxidation of organic matter or biogenic CO_2 dissolution (Liang et al., 2018). Figure 8D

FIGURE 9
Regional distribution of Chloro-Alkaline Indices in the study area.
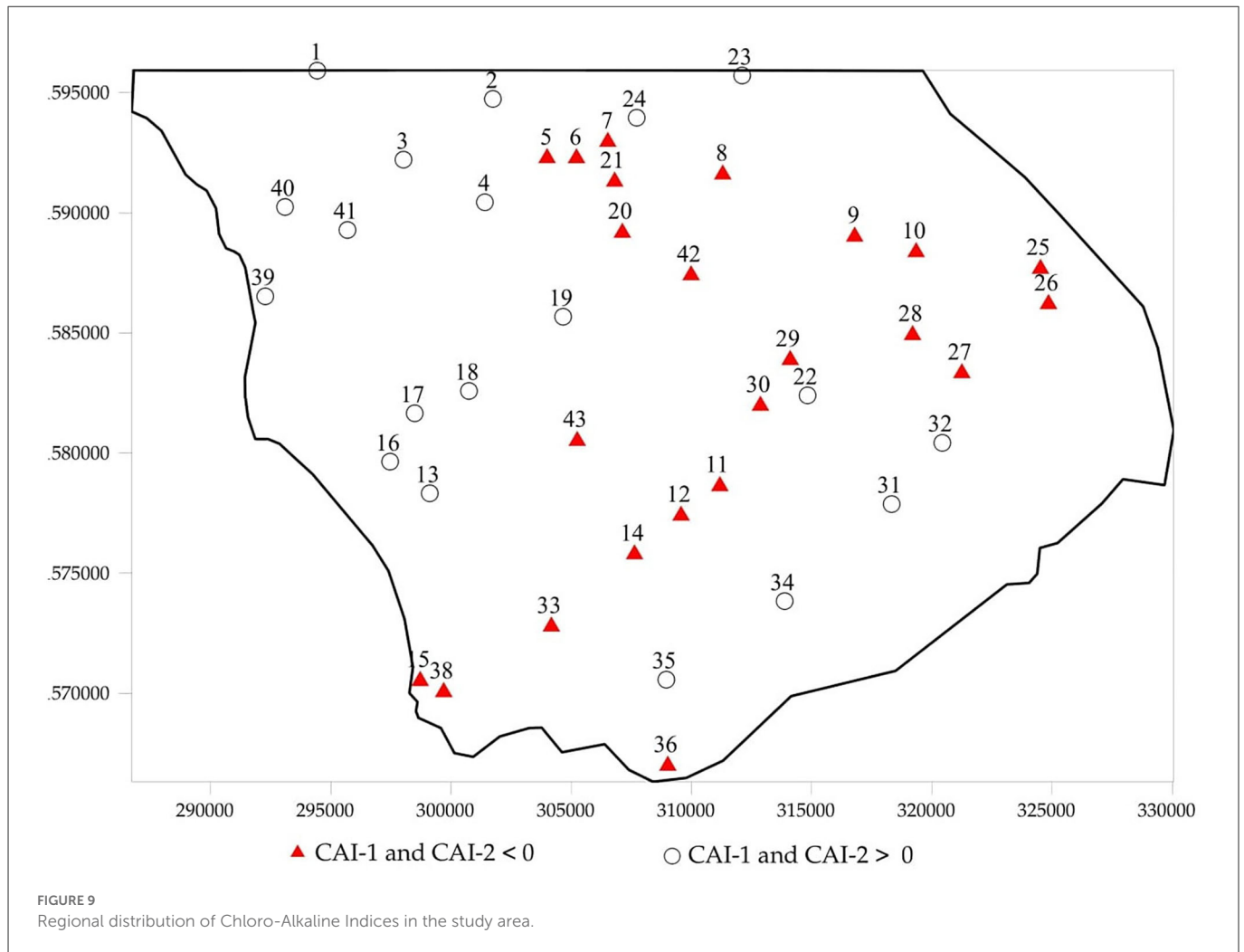
EC vs. Na^+/Cl^- of groundwater samples shows that the trend line has a negative slope revealing a decrease in the Na^+/Cl^- ratio with increasing salinity (EC). This plot indicates the removal of sodium by ion-exchange reaction (Subramani et al., 2009).

Indices of base exchange

Na-Ca exchange is a significant process that can modify cation concentrations in groundwater and influence the evolution of hydrochemical compositions. When the chloroalkaline indices (CAIs) are positive, they indicate an exchange of Na^+ and K^+ from the water with Mg^{2+} and Ca^{2+} from the rocks (base-exchange reaction). It is reversed when CAIs are negative. The chloroalkaline index is observed for 45% of the samples, indicating the exchange of Na^+ and K^+ against the Ca^{2+} and Mg^{2+} ions of the aquifer rocks. The map of the distribution of chloroalkaline indices values (Figure 9) shows that negative values were observed in wells located in a central south-north band and in the north-eastern part of the study area. This observation indicates that the normal ion exchange and reverse ion exchange are geochemical processes controlling the composition of groundwater in a normal scenario. In this study, the pressure of marine waters close to the region modifies the chemical process of groundwaters.

Conclusion

Hydrogeochemical studies were carried out in the central west area of Senegal to (1) identify water quality degradation in the coastal aquifer, (2) estimate its spatial progression, and (3) assess the main geochemical processes responsible for groundwater chemistry using the Piper and Chadha diagrams, chloroalkaline indices, normalized bivariate plots, and multivariate statistical (hierarchical cluster analyses) techniques. The main conclusions are as follows:

- The values of pH indicate a neutral to slightly alkaline water. Electrical conductivity is highly variable, showing very heterogeneous water chemistry.
- The main water type in the region is the $Ca-Mg-HCO_3$ type in the eastern sector, which gradually degrades to a mixed Ca-Mg-Cl type in the central part and then a more saline NaCl type toward the coast.

The HCA gives better precision on the distribution of facies and shows a strong chemical heterogeneity of the waters with several clusters (C_1, C_2, and C_3) and water subclusters (C_{1-1}, C_{1-2}, C_{3-1}, and C_{3-2}). It corresponds to the progression of the saline front that modifies locally the natural interaction between rocks and freshwaters:

- Water–rock interaction is the dominant geochemical process. The silicate weathering, dissolution of carbonates and evaporate, and ion exchanges between water and minerals control the groundwater chemistry. Saline intrusion is also very evident in the area with degradation of groundwater quality.
- The information obtained from the results will be useful for the management of groundwater resources, especially with regard to saltwater intrusion and its progression. A report has been addressed to the stakeholders for preventive actions.
- For future studies, it is envisaged that isotope and dating water will be used to improve understanding of the hydrogeological behavior of the system. Geophysical surveys are underway to better delineate the aquifers in the region. This will allow us to build a quantitative hydrogeological model for the evaluation of the available groundwater resources.

Data quality control

The samples (collection, transport, storage, and preparation before analysis) were managed according to ISO 5667-1, -3, -11, -14, and -22. Major and minor ion analyses by ICP-MS were validated after three measurements/sample. The sensitivity of the ICPMS is determined weekly by fixed concentration standards. During the ICPMS analysis of the samples, blanks are done at the beginning and end of each analytical run. All samples were spiked previously before the analysis with 1 ml of a standard solution (Multielement Standard Solution 6 for ICP, ref 43843-100ML from Thermofisher, ref). All of these procedures allow for the quality assurance of the chemical measurements made in this study.

Data availability statement

The original contributions presented in the study are included in the article/Supplementary material, further inquiries can be directed to the corresponding author.

Author contributions

SN conducted sampling analysis and exploitation of the data and wrote the original version. MD assisted SN on the field and data analysis. SF supervised the research. HC supervised the analysis in his laboratory and the validation of the data and also provided advertisement and modification on the original version. MB corrected the English and also modified parts of the manuscript. PL supervised the different version and made modification before the submission. All authors contributed to the article and approved the submitted version.

Conflict of interest

The authors declare that the research was conducted in the absence of any commercial or financial relationships that could be construed as a potential conflict of interest.

Publisher's note

All claims expressed in this article are solely those of the authors and do not necessarily represent those of their affiliated organizations, or those of the publisher, the editors and the reviewers. Any product that may be evaluated in this article, or claim that may be made by its manufacturer, is not guaranteed or endorsed by the publisher.

Supplementary material

The Supplementary Material for this article can be found online at: https://www.frontiersin.org/articles/10.3389/frwa.2022.1097396/full#supplementary-material

References

Adimalla, N., Li, P., and Qian, H. (2019). Evaluation of groundwater contamination for fluoride and nitrate in semi-arid region of Nirmal Province, South India: a special emphasis on human health risk assessment (HHRA). *Hum. Ecol. Risk Assess.* 25, 1107–1124. doi: 10.1080/10807039.2018.1460579

Adimalla, N., Qian, H., and Nandan, M. J. (2020). Groundwater chemistry integrating the pollution index of groundwater and evaluation of potential human health risk: a case study from hard rock terrain of south India. *Ecotoxicol. Environ. Saf.* 206, 111217. doi: 10.1016/j.ecoenv.2020.111217

Afsari, N., Murshed, S. B., Uddin, S. M. N., and Hasan, M. (2022). Opportunities and Barriers Against Successive Implementation of Rainwater Harvesting Options to Ensure Water Security in Southwestern Coastal Region of Bangladesh. *Front. Water* 4, 811918. doi: 10.3389/frwa.2022.811918

ANSD (2013). *Recensement Général de la Population et de l'Habitat, de l'Agriculture et de l'Elevage*. Rapport définitif 2013, Ministère de l'Economie, des Finances et du Plan du Sénégal.

ARLAB (1982). *Alimentation en eau des Industries Chimiques Sénégalaises. Etude complémentaire du "Maestrichtien"*. Rapport final no 183/3, Dir. Et. Hydr. *Dakar*103p.

Asmael, N. M., Huneau, F., Garel, E., Celle-Jeanton, H., Le Coustumer, P., Dupuy, A., et al. (2015). Origin and recharge mechanisms of groundwater in the upper part of the Awaj River (Syria) based on hydrochemistry and environmental isotope techniques. *Arab. J. Geosci. Saudi Soc. Geosci.* 8, 10521–10542. doi: 10.1007/s12517-015-1953-x

Belkhiri, L., Boudoukha, A., Mouni, L., and Baouz, T. (2010). Application of multivariate statistical methods and inverse geochemical modeling for characterization of groundwater- a case study: Ain Azel plain (Algeria). *Gepoderma* 159, 390–398. doi: 10.1016/j.geoderma.2010.08.016

Belkhiri, L., Mouni, L., and Boudoukha, A. (2012). Evolution of groundwater in an alluvial aquifer: Case of El Eulma aquifer, East Algeria. *J. Afr. Earth Sci.* 66–67, 46–55. doi: 10.1016/j.jafrearsci.2012.03.001

Brahman, K. D., Kazi, T. G., Afridi, H. I., Naseem, S., Arain, S. S., and Ullah, N. (2013). Evaluation of high levels of fluoride, arsenic species and other

physicochemical parameters in underground water of two sub districts of Tharparkar, Pakistan: a multivariate study. *Water Res.* 47, 1005–1020 doi: 10.1016/j.watres.2012.10.042

Brown, C. (1998). *Applied Multivariate Statistics in Geohydrology and Related Sciences*. Springer Science and Business Media. doi: 10.1007/978-3-642-80328-4

Chadha, D. K. (1999). A proposed new diagram for geochemical classification of natural waters and interpretation of chemical data. *Hydrogeol. J.* 7, 431–439 doi: 10.1007/s100400050216

Chebbah, M., and Allia, Z. (2015). Geochemistry and hydrogeochemical process of groundwater in the soouf valley of low Septentrional Sahar, Algeria. *Afr. J. Environ. Sci. Technol.* 9, 261–273. doi: 10.5897/AJEST2014.1710

Chucuya, S., Vera, A., Pino-Vargas, E., Steenken, A., Mahlknecht, J., and Montalván, I. (2022). Hydrogeochemical characterization and identification of factors influencing groundwater quality in coastal aquifers, case: La Yarada, Tacna, Peru. *Int. J. Environ. Res. Public Health* 19, 2815. doi: 10.3390/ijerph19052815

Cloutier, V., Lefebvre, R., Therrien, R., and Savard, M. M. (2008). Multivariate statistical analysis of geochemical data as indicative of the hydrogeochemical evolution of groundwater in a sedimentary rock aquifer system. *J. Hydrol.* 353, 294–313. doi: 10.1016/j.jhydrol.2008.02.015

Datta, P. S., and Tyagi, S. K. (1996). Major ion chemistry of groundwater in Delhi area: chemical weathering processes and groundwater regime. *J. Geol. Soc. India* 47, 179–188.

Dehoorne, O., and Diagne, A. K. (2008). Tourisme, développement et enjeux politiques: l'exemple de la Petite Côte (Sénégal). *Études Caribéennes.* 2008, 9–10. doi: 10.4000/etudescaribeennes.1172

Farnham, I. M., Stetzenbach, K. J., Singh, A. K., and Johannesson, K. H. (2000). Deciphering groundwater flow systems in Oasis valley, Nevada, using trace element chemistry, multivariate statistics, and geographical information system. *Math. Geol.* 32, 943–968. doi: 10.1023/A:1007522519268

Faye, S., Cisse Faye, S., Ndoye, S., and Faye, A. (2003). Hydrogeochemistry of the Saloum (Senegal) superficial coastal aquifer. *Environ. Geol.* 44, 127–136. doi: 10.1007/s00254-002-0749-y

Flicoteaux, R., and et Lappartient, J. P. (1972). Le passage de l'Eocène inferieur à l'Eocène moyen sur la bordure orientale du dôme de NDiass (Sénégal occidental). *Travaux Lab. Sci. Terre, St-Jérôme, Marseille (A),* 6, 1–28.

Freeze, R. A., and Cherry, J. (1979). *Groundwater*. Englewood Cliffs, NJ: Prentice-Hall.

Gaillardet, J., Dupre, B., Louvat, P., and Allegre, C. J. (1999). Global silicate weathering and CO consumption rates deduced 2 from the chemistry of large rivers. *Chem. Geol.* 159, 3–30 doi: 10.1016/S0009-2541(99)00031-5

Gain, A. K., Giupponi, C., and Renaud, F. G. (2012). Climate change adaptation and vulnerability assessment of water resources systems in developing countries: a generalized framework and a feasibility study in Bangladesh. *Water* 4, 345–366. doi: 10.3390/w4020345

Gaye, A. T., and Sylla, M. B. (2018). *Scenarios climatiques au Sénégal. Laboratoire de Physique de l'atmosphère et de l'océan S F (LPAO-SF)*. Rapport, Ecole Supérieure Polytechnique Université Cheikh Anta Diop, Dakar, Sénégal.

Geohydraulique and OMS (1972). *Approvisionnement en eau et assainissements de Dakar et ses environs. Etude des eaux souterraines*. Projet Sénégal 3201 (EX 22), Tome II et III.

Grande, J. A., Borrego, J., Torre, M. L. D., and Sainz, A. (2003). Application of cluster analysis to the geochemistry zonation of the estuary waters in the Tinto and Odiel rivers (Huelva, Spain). *Environ. Geochem. Health* 25, 233–246. doi: 10.1023/A:1023217318890

Güler, C., and Thyne, G. D. (2004). Hydrologic and geologic factors controlling surface and groundwater chemistry in Indian Wells–Owens valley area, southeastern California, USA. *J. Hydrol.* 285, 177–198. doi: 10.1016/j.jhydrol.2003.08.019

Güler, C., Thyne, G. D., McCray, J. E., and Turner, A. K. (2002). Evaluation of graphical and multivariate statistical methods for classification of water chemistry data. *Hydrogeology* 10, 455–474. doi: 10.1007/s10040-002-0196-6

Helstrup, T., Jorgensen, N. O., and Banoeng-Yakubo, B. (2007). Investigation of hydrochemical characteristics of groundwater from Cretaceous–Eocene limestone aquifers in southern Ghana and Togo using hierarchical cluster analysis. *Hydrogeol. J.* 15, 977–989. doi: 10.1007/s10040-007-0165-1

Hem, J. D. (1992). *Study and Interpretation of Chemical Characteristics of Natural Water*, 3rd Edn. USGS Water-Supply Paper, 2254.

Hussain, M. S., Abdelhamid, H. F., Javadi, A. A., and Mohsen, M. S. (2019). Management of seawater intrusion in coastal aquifers: a review. *Water* 11, 2467. doi: 10.3390/w11122467

Hussein, M. T. (2004). Hydrochemical evaluation of groundwater in the Blue Nile Basin, eastern Sudan, using conventional and multivariate techniques. *Hydrogeol. J.* 12, 144–158. doi: 10.1007/s10040-003-0265-5

Hussien, B. M., and Faiyad, A. S. (2016). Modeling the hydrogeochemical processes and source of ions in the groundwater of aquifers within Kasra-Nukhaib Region (West Iraq). *Int. J. Geosci.* 7, 1156–1181. doi: 10.4236/ijg.2016.710087

Kaur, L., Rishi, M. S., and Sharma, S. (2019). Hydrogeochemical characterization of groundwater in alluvial plains of river Yamuna in northern India: an insight of controlling processes. *J. King Saud Univ. Sci.* 31, 1245–1253. doi: 10.1016/j.jksus.2019.01.005

Leroux, M. (1995). La dynamique de la grande sécheresse sahélienne / Dynamics of the Great Sahelian Drought. *Rev. Géogr. Lyon* 70, 223–232. doi: 10.3406/geoca.1995.4216

Li, C., Men, B. H., and Yin, S. Y. (2022). Analysis of groundwater chemical characteristics and spatiotemporal evolution trends of influencing factors in southern Beijing Plain. *Front. Environ. Sci.* 10, 913542. doi: 10.3389/fenvs.2022.913542

Liang, Z., Chen, J., Jiang, T., Kun, L., Gao, L., Wang, Z., et al. (2018). Identification of the dominant hydrogeochemical processes and characterization of potential contaminants in groundwater in Qingyuan, China, by multivariate statistical analysis. *RSC Adv.* 8, 33243. doi: 10.1039/C8RA06051G

Madioune, D. H., Faye, S., Orban, P., Brouyère, S., Dassargues, A., Mudry, J., et al. (2014). Application of isotopic tracers as a tool for understanding hydrodynamic behavior of the highly exploited Diass aquifer system (Senegal). *J. Hydrol.* 511 443–459. doi: 10.1016/j.jhydrol.2014.01.037

Magha, A., Awah, M., Nono, G., Tamfuh, P., Wotchoko, P., Adoh, M., et al. (2021). Assessment of groundwater quality for domestic and irrigation purposes in northern Bamenda (Cameroon). *J. Water Resour. Prot.* 13, 1–19. doi: 10.4236/jwarp.2021.131001

Maignien, R. (1965). *Carte pédologique du Sénégal au 1/1000000*. Notice Explicative. ORSTOM Dakar.

Marghade, D. (2020). Detailed geochemical assessment and indexing of shallow groundwater resources in metropolitan city of Nagpur (western Maharashtra, India) with potential health risk assessment of nitrate enriched groundwater for sustainable development (2020) Chemie der Erde. *Geochemistry* 80, 125627. doi: 10.1016/j.chemer.2020.125627

Melloul, A., and Collin, M. (1992). The 'principal components' statistical method as a complementary approach to geochemical methods in water quality factor identification; application to the Coastal Plain aquifer of Israel. *J. Hydrol.* 140, 49–73. doi: 10.1016/0022-1694(92)90234-M

Monciardini, C. (1966). La sédimentation éocène au Sénégal. *Mem. Bur. Rech. Geol. Min. Orleans* 43, 65.

Montcoudiol, N., Molson, J., Lemieux, J.-M. (2014). Groundwater geochemistry of the Outaouais Region (Québec, Canada): a regional-scale study. *Hydrogeol. J.* 23, 377–396. doi: 10.1007/s10040-014-1190-5

Mudry, J., and Travi, Y. (1995). "Enregistreurs et indicateurs de l'évolution de l'environnement en zone tropicale," in *Sécheresse Sahélienne et Action Anthropique - Deux Facteurs Conjugués de Dégradation des Ressources en eau de l'Afrique de l'Ouest - Exemple du Sénégal, P.*, eds R. Maire, S. Pomel, and J.-N. Salomon (Univ. Bordeaux), 219–234. doi: 10.4000/books.pub.10172

Mufur, A. M., Awah, M. T., Tamfuh, P. A., Agendia, M. A., Ngambu, A. A., and Kabeyene, V. K. (2021). Groundwater resources for domestic and irrigation purposes in Melong (Littoral Region, Cameroon): hydrogeochemical constraints. *Afr. J. Environ. Sci. Technol.* 15, 270–281. doi: 10.5897/AJEST2021.3027

Ndoye, S., Fontaine, C., Gaye, C. B., and Razack, M. (2018). Groundwater quality and suitability for different uses in the saloum area of Senegal. *Water* 10, 1837. doi: 10.3390/w10121837

Paul, R., Brindha, K., Gowrisankar, G., Tan, M. L., and Singh, M. K. (2019). Identification of hydrogeochemical processes controlling groundwater quality in Tripura, Northeast India using evaluation indices, GIS, and multivariate statistical methods. *Environ. Earth Sci.* 78, 470. doi: 10.1007/s12665-019-8479-6

Perez Villarreal, J., Avila Olivera, J. A., Israde Alcantara, I., and Buenrostro Delgado, O. (2019). Nitrate as a parameter for differentiating groundwater flow systems in urban and agricultural areas: the case of Morelia-Capula area, Mexico. *Hydrogeol. J.* 27, 1767–1778. doi: 10.1007/s10040-019-01933-0

Piper, A. M. (1944). A graphic procedure in the chemical interpretation of water analysis. *Am. Geophys. Union Trans.* 25, 914–923. doi: 10.1029/TR025i006p00914

Raza, M., Farooqi, A., Niazi, N. K., and Ahmad, A. (2016). Geochemical control on spatial variability of fluoride concentrations in groundwater from rural areas of Gujrat in Punjab, Pakistan. *Environ. Earth Sci.* 75, 1364. doi: 10.1007/s12665-016-6155-7

Razack, M., Jalludin, M., and Gaba, A. H. (2019). Simulation of climate change impact on a coastal aquifer under arid climate. The Tadjourah Aquifer (Republic of Djibouti, Horn of Africa). *Water* 11, 2347. doi: 10.3390/w11112347

Ren, X., Yu, R., Kang, J., Li, X., Wang, R., Zhuang, S., et al. (2022). Hydrochemical evaluation of water quality and its influencing factors in a closed inland lake basin of Northern China. *Front. Ecol. Evol.* 10, 1005289. doi: 10.3389/fevo.2022.1005289

Saha, N., and Safiur Rahman, M. (2020). Groundwater hydrogeochemistry and probabilistic health risk assessment through exposure to arsenic-contaminated groundwater of Meghna floodplain, central-east Bangladesh. *Ecotoxicol. Environ. Saf.* 206, 111349. doi: 10.1016/j.ecoenv.2020.111349

Saint-Marc, P., and Sarr, R. (1984). Précisions biostratigraphiques et paléo environnementales sur le sommet du Paléocène et la base de l'Eocène de la région de Mbour-Joal (Sénégal). *Jour. Afric. Earth Sci.* 2, 203–207. doi: 10.1016/S0731-7247(84)80015-4

Sarr, R. (1982). *Etude géologique et hydrogéologique de la région de Joal-Fadiouth (Sénégal)*. Thèse 3ème cycle, Univ. Dakar (1982), 166.

Sarr, R. (1999). Le Paléogène de la région de Mbour-Joal (Sénégal occidental) : biostratigraphie, étude systématique des ostracodes, paléoenvironnement. *Rev. Paléobiol. Genève* 18, 1–29.

Schoeller, H. (1934). Les échanges de base dans les eaux souterraines; trois exemples en Tunisie. *Bull. Soc. Geol. Fr.* 4, 389–420.

Schoeller, H. (1967). *Geochemistry of Groundwater-an International Guide for Research and Practice, Chap. 15.* UNESCO, 1–18.

Simler, R. (2009). *Diagrammes.* Avignon, France: Laboratoire d'Hydrogéologie d'Avignon.

StatSoft Inc. (2004). *STATISTICA (data analysis software system), version 7.* Available online at: https://www.statistica.com/en/ (accessed January 14, 2023).

Su, C., Liu, Y., Cheng, Z., Wang, W., and Zheng, Z. (2022), Hydrochemical process and controls on the hydrochemistry of river water in the Muling-Xingkai Plain, Northeast China. *Front. Environ. Sci.* 10, 1010367. doi: 10.3389/fenvs.2022.1010367

Su, Y., Zhu, G., Feng, Q., Li, Z., and Zhang, F. (2009). Environmental isotopic and hydrochemical study of groundwater in the Ejina Basin, northwest China. *Environ. Geol.* 58, 601–614. doi: 10.1007/s00254-008-1534-3

Subramani, T., Rajmohan, N., and Elango, L. (2009). Groundwater geochemistry and identification of hydrogeochemical processes in a hard rock region, Southern India. *Environ. Monit. Assess.* 34, 35–37. doi: 10.1007/s10661-009-0781-4

Tessier, F. (1954). Contribution à la stratigraphie et à la paléontologie de la partie ouest du Sénégal (Crétacé et Tertiaire). *Bull. Dir. Mines Afr. Occid.* 14, 570.

Tine, A. K., Ba, M. I., Gladima–Siby, A. S., Essouli, O. F., Faye, A., and Sarr, B. (2011). Actualization of the Maastrichtian and Paleocene aquifers hydrogeological situation of the region of Mbour, Senegal. *J. Sci. Technol.* 9, 23–32.

Travi, Y. (1988). *Hydrogéochimie et hydrogéologie des aquifères fluorés du bassin du Sénégal. Origine et conditions de transport du fluor dans les eaux souterraines. Thèse Sciences.* Univ. de Paris Sud (Orsay), 190.

Travi, Y., Sarr, R., Faye, A., and Gaye, C.-B. (1983). Etude chimique de l'évolution du front salé de la nappe paléocène de la région de Mbour. *Rapport Inédit.* 3A-82-4713, 1–25.

Wang, H. X., Jiang, W., Wan, L., Guilin, H.an, and Guo, H. (2015). Hydrogeochemical characterization of groundwater flow systems in the discharge area of a river basin. *J. Hydrol.* 527, 433–441. doi: 10.1016/j.jhydrol.2015.04.063

Wang, P., Yu, J., Zhang, Y., and Liu, C. (2013). Groundwater recharge and hydrogeochemical evolution in the Ejina Basin, northwest China. *J. Hydrol.* 476, 72–86. doi: 10.1016/j.jhydrol.2012.10.049

Wang, X., Geng, X., Sadat-Noori, M., and Zhang, Y. (2022). Groundwater-Seawater Exchange and Environmental Impacts. *Front. Water* 4, 928615. doi: 10.3389/frwa.2022.928615

WHO (2011). *Guideline for Drinking-Water Quality, 4th Edn.* Geneva, SwitzerlandL World Health Organization.

Winter, T. C., Harve, W. J., Franke, O. L., and Alley, W. M. (1998). *Ground Water and Surface Water: A Single Resource.* Denver, Colorado: US Geological Survey Circular, 1139, 87 p. Available online at: http://pubs.usgs.gov/circ/circ1139/index.html (accessed January 14, 2023).

Wu, C. L. R., Stigter, T. Y., and Craig, S. G. (2022). Assessing the quantity and quality controls of the freshwater lens on a semi-arid coral-limestone Island in Sri Lanka. *Front. Water* 4, 832227. doi: 10.3389/frwa.2022.832227

Yao, R., Yan, Y., Wei, C., Luo, M., Xiao, Y., and Zhang, Y. (2022). Hydrochemical characteristics and groundwater quality assessment using an integrated approach of the PCA, SOM, and Fuzzy c-means clustering: a case study in the northern Sichuan Basin. *Front. Environ. Sci.* 10, 907872. doi: 10.3389/fenvs.2022.907872

Yidana, S. M., Ophori, D., and Banoeng-Yakubo, B. (2008). Hydrogeological and hydrochemical characterization of the Voltaian Basin: the Afram Plains area, Ghana. *Environ. Geol.* 53, 1213–1223. doi: 10.1007/s00254-007-0710-1

Yousfi, Y., El, H.imi, M., Ouarghi, H., El, Elgettafi, M., Benyoussef, S., Gueddari, H., et al. (2002). Hydrogeochemical and statistical approach to characterize groundwater salinity in the Ghiss-Nekkor coastal aquifers in the Al Hoceima province, Morocco. *Groundwater Sust. Dev.* 19, 100818. doi: 10.1016/j.gsd.2022.100818

Zhou, Y., Li, P., Xue, L., Dong, Z., and Li, D. (2020). Solute geochemistry and groundwater quality for drinking and irrigation purposes: a case study in Xinle city. *Geochemistry* 80, 125609. doi: 10.1016/j.chemer.2020.125609